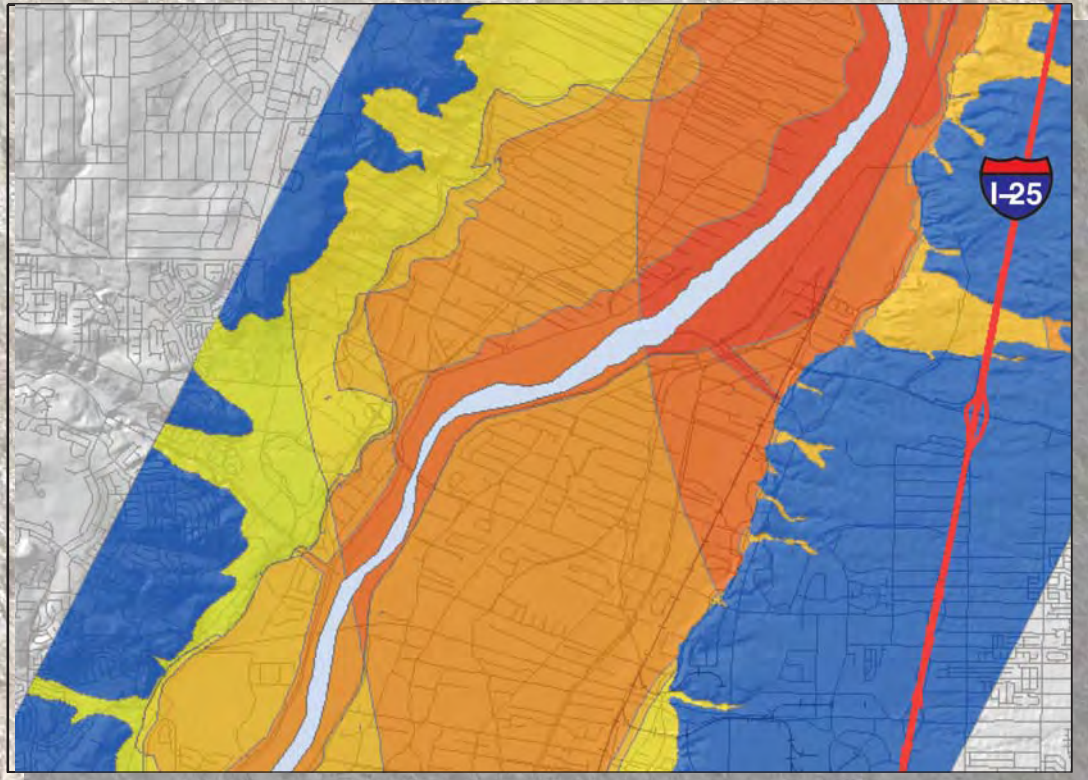


Final Technical Report

GIS-based Liquefaction Potential and Effects Mapping, Albuquerque-Santa Fe Corridor, New Mexico



Submitted to:

U. S. Geological Survey
National Earthquake Reduction Program
Award Number 03HQGR0067

Submitted by:

William Lettis & Associates, Inc.
1777 Botelho Drive, Suite 262
Walnut Creek, CA 94596

April 2007

FINAL TECHNICAL REPORT

**GIS-BASED LIQUEFACTION POTENTIAL AND EFFECTS MAPPING,
ALBUQUERQUE-SANTA FE CORRIDOR, NEW MEXICO**

By:

Christopher Hitchcock and Keith Kelson
William Lettis & Associates, Inc.
1777 Botelho Drive, Suite 262, Walnut Creek, CA 94596
(925) 256-6070; hitch@lettis.com

Digital database developed by:

Christopher Hitchcock, Robert Givler, and Justin Pearce
William Lettis & Associates, Inc.

Program Elements: I, II

Recipient: William Lettis & Associates, Inc.

Principal Investigators: Christopher S. Hitchcock and Keith I. Kelson

**National Earthquake Hazards Reduction Program
U.S. Geological Survey Award Number 03-HQ-GR-0067**

Research supported by the U.S. Geological Survey (USGS), Department of the Interior, under USGS award number 03-HQ-GR-0067. The views and conclusions contained in this document are those of the authors and should not be interpreted as necessarily representing the official policies, either expressed or implied, of the U.S. Government.

April 2007

GIS-Based Liquefaction Potential and Effects Mapping, Albuquerque-Santa Fe Corridor, New Mexico

Christopher S. Hitchcock and Keith I. Kelson
William Lettis & Associates, Inc.
1777 Botelho Drive, Suite 262, Walnut Creek, CA 94596
(925) 256-6070; hitch@lettis.com

U.S. Geological Survey
National Hazard Reduction Program

Program Element I and II: *I: Products for Earthquake Loss Reduction (90%); II: Research on Earthquake Physics and Effects (10%)*

Key Words: Liquefaction, Susceptibility, Zonation, Seismic Hazard

ABSTRACT

Based on our previous NEHRP-funded liquefaction susceptibility mapping, large areas of the inner Rio Grande valley within the metropolitan Albuquerque area are susceptible to liquefaction (Kelson et al., 1999; Kelson et al., 2000). Evidence exists for the occurrence of large surface-rupturing earthquakes of magnitude (M) 7 on major faults in the Albuquerque area (Kelson et al., 1998; Personius et al, 2001) with the potential for generating high ground motions (Wong et. al., 2004). We have integrated our existing NEHRP-funded liquefaction susceptibility maps (Kelson et al., 1999) with NEHRP-funded ground motion potential maps (Wong et al, 2000; Wong et al, 2004) to prepare liquefaction potential maps. The maps cover approximately 300 square kilometers of the Rio Grande Valley, and include the metropolitan Albuquerque area, river front communities between Bernalillo and Isleta Pueblo, and areas of industrialization in the heart of the Albuquerque-Santa Fe corridor. The maps depict the potential for liquefaction within 500- and 2,500-year return periods and for a M7.0 scenario earthquake on the Sandia-Rincon fault. In addition, we have applied established quantitative techniques for estimating the locations and magnitudes of possible liquefaction-related ground failures to generate maps of possible liquefaction-related permanent ground deformation (PGD), including ground settlement and lateral spreads, for the metropolitan downtown Albuquerque area.

Our final map products include GIS layers for input into the City of Albuquerque and Bernalillo County GIS to address the present need for interactive hazard mapping tools for earthquake mitigation and response in the metropolitan Albuquerque area. GIS map layers from this study show the following:

- Potential for liquefaction within deposits present beneath the metropolitan Albuquerque area within 500- and 2,500-year return periods;
- Potential for liquefaction within deposits present beneath the metropolitan Albuquerque area associated with a M7.0 earthquake on the Sandia-Rincon fault;
- Potential for ground settlement (including isopach maps of potential settlement); and
- Potential for lateral ground displacement (including likely locations and estimated amounts of lateral spreads).

TABLE OF CONTENTS

Abstract.....	i
Table of Contents.....	ii
1.0 INTRODUCTION.....	1
2.0 GEOLOGIC SETTING	3
3.0 PREVIOUS WORK	5
3.1 Liquefaction Susceptibility Maps.....	5
3.2 Earthquake Scenario and Probabilistic Ground Motion Maps.....	9
4.0 LIQUEFACTION POTENTIAL MAPS	10
4.1 Scenario-based Liquefaction Potential	11
4.2 Probabilistic-based Liquefaction Potential	13
5.0 PERMANENT GROUND DEFORMATION (PGD) MAPS	18
5.1 Ground Settlement.....	18
5.2 Lateral Spread.....	19
6.0 DISCUSSION	21
7.0 SUMMARY	22
8.0 ACKNOWLEDGMENTS.....	23
9.0 REFERENCES.....	24

List of Figures

1 Location map showing area of study.....	4
2 Map of major faults in vicinity of study area.....	8
3 Conceptual diagram showing integration of liquefaction susceptibility mapping with ground shaking mapping.....	12
4 Map showing potential settlement for downtown Albuquerque.....	18

List of Plates

1 Surficial Geologic Map
2 Liquefaction Susceptibility Map
3 Scenario-based Liquefaction Potential Map (Sandia-Rincon fault)
4 Probabilistic Liquefaction Potential Map – 2% Probability of Exceedance in 50 years
5 Probabilistic Liquefaction Potential Map – 10% Probability of Exceedance in 50 years

The consequences of a large earthquake in the vicinity of the Albuquerque metropolitan area would be significant, in part because of the high likelihood of liquefaction-related ground failures in the inner Rio Grande valley. The inner Rio Grande valley includes metropolitan Albuquerque as well as critical lifelines and facilities supporting the largest population center in the State of New Mexico (Figure 1). Our previous NEHRP-funded liquefaction susceptibility mapping showed that most of the inner valley is underlain by sediments with high or very high susceptibility to liquefaction (Kelson et al., 1999, 2000). Overall, it is reasonable to assume that roughly 240 square kilometers (90 square miles) along the Rio Grande could experience liquefaction-related damage resulting from a moderate to large earthquake on any of several nearby late Quaternary faults. Along with damage to buildings, vital bridges, and other infrastructure, liquefaction-related failure of river levees in the inner Rio Grande valley may cause localized flooding.

The potential for liquefaction depends on not only the *susceptibility* of a deposit to liquefy but also the *opportunity* for ground motions to exceed a specified threshold level required for initiation of liquefaction. Albuquerque is located in the seismically active Rio Grande rift, which contains north-striking, late Quaternary normal faults that are potential seismic sources (Figure 2). These sources include the Sandia-Rincon fault along the western margin of the Sandia Mountains, the West Mesa fault zone west of the Rio Grande, and the Hubbell Spring fault bordering the Manzanita and Manzano Mountains (Figure 2; Wong et al., 1996; Connell, 1997; Machette et al., 1998). Recent paleoseismic studies suggest that, although infrequent, several major faults in the Albuquerque area have experienced large earthquakes in the late Holocene (Machette et al., 1998; Personius et al., 1999, 2001). These data provide direct evidence for the possible future occurrence of large earthquakes of magnitude 7 or greater in the Albuquerque area, despite the scarcity of moderate to large historical earthquakes (Wong et al., 2004).

We have integrated our existing NEHRP-funded liquefaction susceptibility maps (Kelson et al., 1999) with NEHRP-funded ground motion potential maps (Wong et al., 2004) to prepare liquefaction potential maps. For this project, we digitized the surficial geologic and liquefaction susceptibility maps produced for NEHRP by Kelson et al. (1999). We used these maps, with ground motion maps produced for the Albuquerque-Santa Fe corridor by Wong et al. (2000, 2004), to produce liquefaction potential maps. The maps cover approximately 300 square kilometers of the Rio Grande Valley, and include the metropolitan Albuquerque area, river front communities between Bernalillo and Isleta Pueblo, and areas of industrialization in the heart of the Albuquerque-Santa Fe corridor (Figures 1 and 2). The maps depict the potential for liquefaction for a possible

Mw7.0 earthquake on the Sandia-Rincon fault and for 500- and 2,500-year return periods. Because of the relatively low rate of historic seismicity in the Rio Grande rift, the liquefaction potential maps presented in this report likely more accurately depict the distribution and likely severity of liquefaction hazard in the Albuquerque metropolitan region than the liquefaction susceptibility maps.

Albuquerque is located in the Rio Grande rift in central New Mexico (Figure 1). The eastern margin of the rift is bordered by active and potentially active faults adjacent to the Sandia, Manzanita, and Manzano uplifts. These normal faults (e.g., Sandia/Rincon, Manzano, Hubbell Spring; Figure 2) have more than 10,000 ft (3 km) of down-to-the-west vertical separation, and have exposed Proterozoic rocks in the footwall uplifts.

Within the Rio Grande rift, the Rio Grande River flows from north to south transporting sediments from northern New Mexico and southern Colorado. Geologic mapping by several workers, including Lambert (1968), GRAM/William Lettis & Associates, Inc. (1995), and Connell (1995, 1997, 1998a, 1998b) show that this alluvium is inset into Pleistocene alluvium, alluvial-fan deposits and Tertiary bedrock that comprise the adjacent piedmont slopes. Holocene and alluvial-fan deposits derived from arroyos draining the piedmonts west and east of the inner valley interfinger with Rio Grande fluvial deposits. The inner Rio Grande valley is underlain primarily by saturated, unconsolidated sandy alluvium deposited by the Rio Grande and tributary arroyos. This alluvium consists predominantly of sand and gravel with discontinuous interbeds of silt and clay. Borehole data from these deposits show that most have low Standard Penetration Test (SPT) blow counts. The valley also contains levees, embankments and other man-made features composed of engineered and non-engineered artificial fill (Kelson et al., 1999). Groundwater in the inner valley is very shallow, with depths beneath most of the valley of less than 12 m (40 ft).

Recent compilations of potential seismic sources in northern New Mexico show the presence of numerous late Quaternary faults and demonstrate that there is a real potential for significant strong ground motion in the Albuquerque region (Wong et al., 1996; Machette et al., 1998; Personius et al., 1999). Paleoseismic studies of major faults in the region suggest that, although infrequent, several major faults in the Albuquerque area have experienced large earthquakes in the late Holocene (Machette et al., 1998; Personius et al., 2001). These data provide direct evidence for the occurrence of large earthquakes of magnitude (M) 7 or greater in the Albuquerque area, despite the scarcity of moderate and large historical earthquakes. Intensities associated with moderate pre-instrumental earthquakes (Olsen, 1979) suggest that peak ground accelerations (PGA) in the middle Rio Grande Valley were sufficient to trigger liquefaction in highly susceptible sediments, although no instances of liquefaction or paleoliquefaction have been reported in the literature. Therefore, the geologic evidence of large earthquakes near Albuquerque demonstrates that the opportunity exists to produce liquefaction in susceptible sediments that are present in the Rio Grande valley.

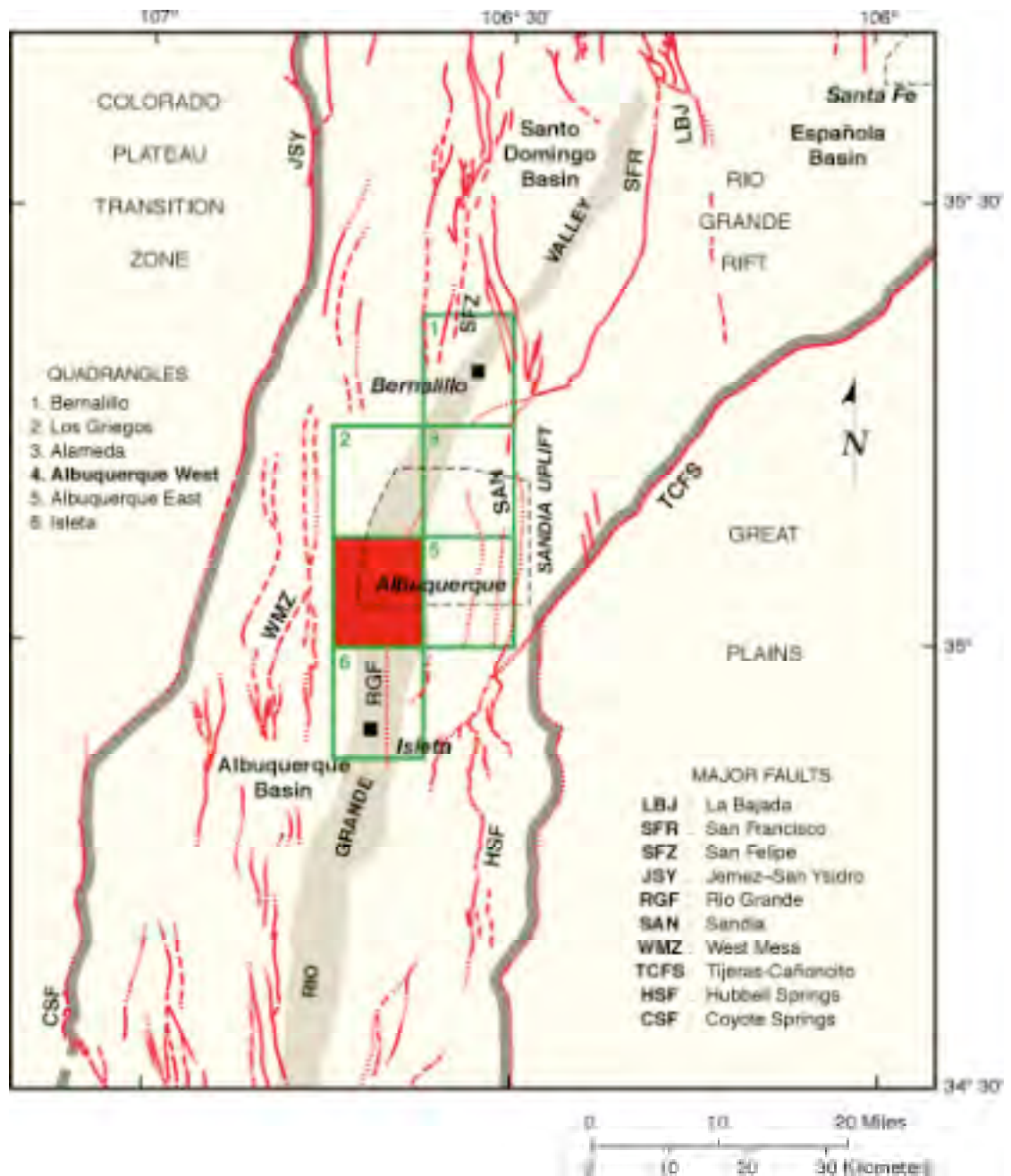


Figure 1. Generalized regional tectonic map of the Rio Grande rift near Santa Fe and Albuquerque showing area of existing liquefaction susceptibility maps (Kelson et al., 1999) and liquefaction potential maps produced for this study. Stippled area shows the inner Rio Grande Valley, which contains saturated Holocene alluvial and eolian sediments. Faults after Machette and McGimsey (1982), Kelson and Hitchcock (1994), and Wong et al. (1996). Detailed liquefaction-related permanent ground deformation maps cover a portion of the Albuquerque West 7.5-minute quadrangle shown in red.

The primary basis for classifying liquefaction susceptibility in the inner Rio Grande Valley is our mapping of late Quaternary deposits, supplemented by quantitative evaluation of geotechnical borehole data (Kelson et al., 1999). Geologic mapping provided a means to extrapolate localized boring log data to areas for which there are few or no subsurface data, thus allowing delineation of liquefaction hazards over large areas. Geologic units mapped on the basis of depositional environment and relative age are particularly useful for estimating lithologic sorting, bedding, grain-size characteristics, and degree of compaction of sedimentary deposits in areas that lack subsurface data.

3.1 Liquefaction Susceptibility Mapping

The first step in regional assessment of the potential for liquefaction is the determination of whether or not soils susceptible to liquefaction are present (Seed and Cetin, 2003). In our previous mapping of liquefaction hazards within the inner Rio Grande Valley (e.g. Figure 2; Kelson et al, 1999), we mapped the distribution of natural and man-made deposits susceptible to liquefaction. Our delineation of late Quaternary deposits involved analysis of aerial photography, field reconnaissance mapping, and synthesis of existing geologic maps, soil surveys, and detailed topographic maps. We also collected information on historical flooding in the inner valley to help delineate historical floodplain deposits.

Geotechnical, environmental, and groundwater boring logs provided lithologic and engineering properties for alluvial deposits in the inner Rio Grande valley. Lithologic properties derived from the boring logs typically include soil color, type, and texture from field observations and laboratory particle-size distribution analyses. Geotechnical properties generally include dry unit weight, penetration resistance, and relative compaction. Standard Penetration Test (SPT) data extracted from boring logs were compiled and digitized for the study area for use in quantitative analyses of liquefaction susceptibility.

Borehole data used to evaluate liquefaction susceptibility included boring logs compiled for our mapping and as part of a Master's thesis by Jodi Clark (New Mexico Tech). We incorporated 159 boring logs that included information on borehole location, grain size distribution, SPT N-values, depth to groundwater, and other data. These data were derived primarily from the New Mexico State Highway and Transportation Department for geotechnical investigations along major highways and bridges in the inner valley. The 159 boring logs represent shallow subsurface

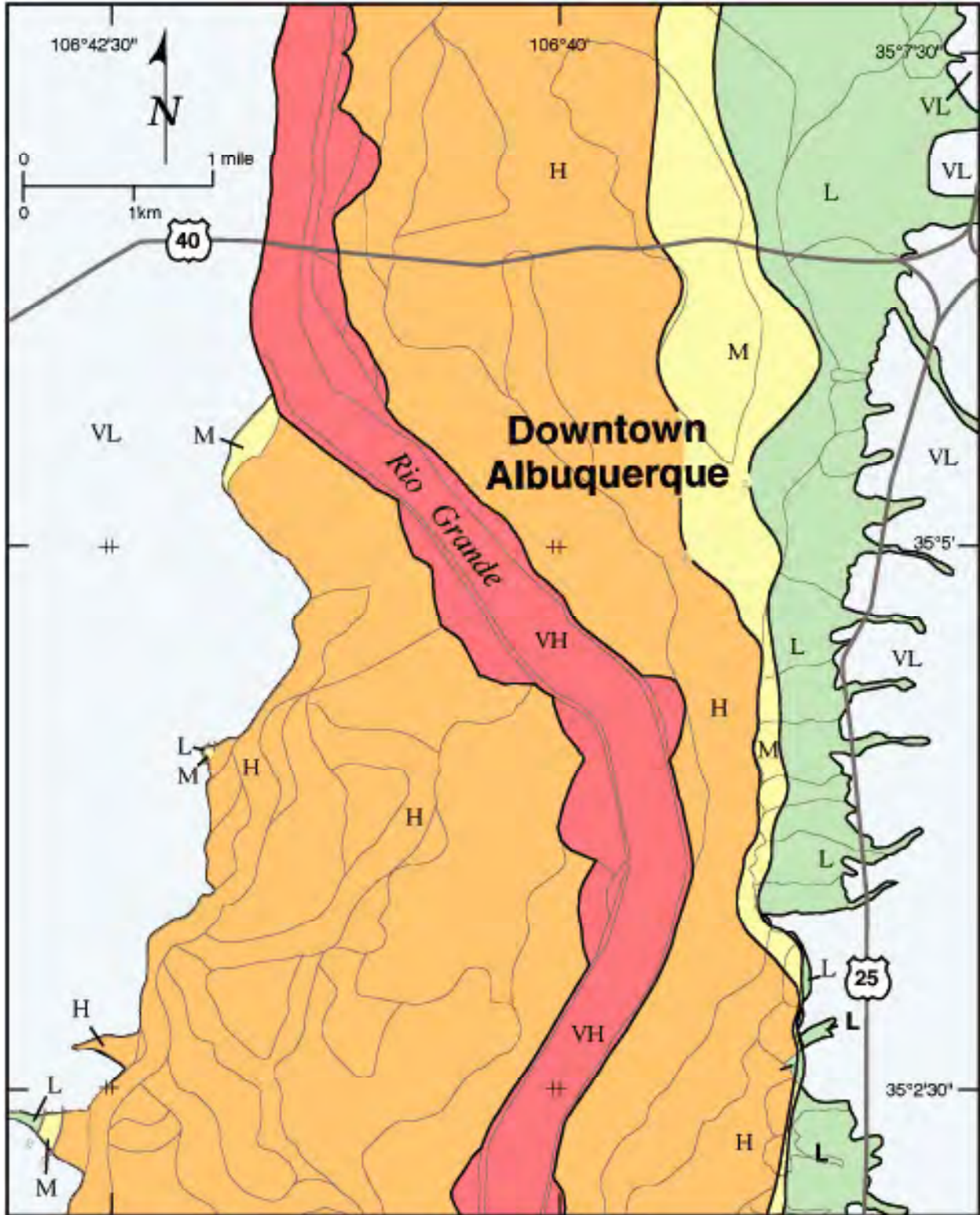


Figure 2. Portion of liquefaction susceptibility map for downtown Albuquerque showing areas of high and very high liquefaction hazard (Kelson et al., 1999).

conditions at approximately 30 sites in the inner valley and adjacent slopes, mostly on the Albuquerque West and Los Griegos quadrangles.

Liquefaction susceptibility was mapped based on three factors: (1) the total thickness of loose sandy deposits within 40 ft (12 m) of the ground surface, (2) the depth of groundwater, and (3) the estimated threshold ground motions required to initiate liquefaction. The threshold ground motions are based on available blow-count data, and calculations using the Seed Simplified Procedure and subsequent revisions (Seed and Idriss, 1971; Seed et al., 1983, 1985; Seed and Harder, 1990; Idriss, 1997; Robertson and Wride, 1997; Youd, 1997). This procedure is based on groundwater conditions, overburden loads, sediment densities from Standard Penetration Testing (SPT), and calculated cyclic stress ratios. SPT and laboratory data derived from shallow boring logs provide the means to establish material strengths and density for mapped geologic deposits. SPT data, in particular, provide a standardized measure of the penetration resistance.

The relative susceptibility of each surficial geologic map unit is based on calculation of the threshold peak ground acceleration (PGA) value required to initiate liquefaction. Our classification of relative liquefaction susceptibility incorporated the “equivalent uniform cyclic stress ratio” (*CSReq*) for the number of earthquake cycles typical of a scenario event of Mw 7.0. The susceptibility classes determined by triggering PGA-threshold values are shown below.

- Very High - may trigger at less than 0.1 g
- High - may trigger between 0.1 g and 0.2 g
- Moderate - may trigger between 0.2 g and 0.3 g
- Low - may trigger at levels above 0.3 g
- Very Low - unlikely to trigger at any level of acceleration

Classification of deposit susceptibility is based on analyses of borehole data in conjunction with geologic information on deposit characteristics (e.g., consolidation, soil development, deposit age) and depths to groundwater. Our assignments of deposits to the liquefaction susceptibility classes are summarized briefly below. On the basis of this classification, we integrated historic groundwater maps with our Quaternary geologic maps (Plate 1) to produce liquefaction susceptibility maps (Plate 2).

Very High liquefaction susceptibility ratings were assigned to saturated deposits determined to have threshold PGA values consistently less than 0.1 g based on analyses of borehole data (Kelson et

al., 1999). In the inner Rio Grande Valley, these deposits include Holocene floodplain deposits (units Qhfpa and Qhfp), which have threshold values ranging from 0.03 to 0.26 g. Although some of the boreholes in floodplain deposits yielded threshold values of more than 0.2 g, the lithologic variability of the alluvial sediments is large and it is appropriate to classify these saturated, unconsolidated sand and gravel deposit as very highly susceptible to liquefaction. Where groundwater is less than 9 m (30 ft) depth, these deposits are classified as having a Very High susceptibility to liquefaction. Where groundwater is greater than 9 m (30 ft), but less than 12 m (40 ft), these deposits are assigned to the High susceptibility class based on the decreased likelihood of liquefaction with deeper groundwater. In addition, a Very High rating is assigned to areas of saturated artificial fill (unit "af"), which includes riverside levees, canal levees, local reservoir embankments, and fill placed for flood control structures, roadways and railroads. Although some of these fills may be engineered and thus may have lower susceptibilities, we conservatively estimate that all artificial fills have Very High susceptibilities.

High susceptibility ratings were assigned to saturated deposits determined to have threshold PGA values less than 0.2 g (Kelson et al., 1999). These deposits include Holocene alluvial valley deposits (units Qha1, Qha2, Qha3 and Qha4), eolian deposits (unit Qhe), and alluvial-fan deposits (units Qhfy and Qhfo) where groundwater is less than 9 m (30 ft) deep (Plate 1). Where groundwater is greater than 9 m (30 ft), but less than 12 m (40 ft), these deposits are assigned to the Moderate susceptibility class, based on the lower likelihood of liquefaction with deeper groundwater. Where groundwater is more than 12 m (40 ft) deep, these deposits are classified as having Low susceptibility (Plate 2).

Moderate susceptibility ratings were assigned to saturated colluvial deposits (unit Qhc) and Pleistocene alluvial-fan deposits (unit Qpf) estimated to have threshold PGA values less than 0.3 g (Kelson et al., 1999). In addition, the Pleistocene alluvial-fan deposits contain moderately developed soil profiles that lessen liquefaction susceptibility. Where groundwater is deeper than 9 m (30 ft), we classified these deposits as having Low susceptibility.

On the basis of high dry density and consolidation values and high blow counts, middle Pleistocene deposits were assigned to the Low and Very Low susceptibility classes (Table 1). A "Low" rating was assigned to map units that pre-date the latest Pleistocene (>15 ka), units that are estimated to not liquefy given 0.3 g or lesser PGA, or areas where groundwater is greater than 40 ft (12 m). Where groundwater is less than 12 m below the ground surface, Pleistocene deposits were assigned to the Low susceptibility class, rather than Very Low, because these map units may contain minor areas of unconsolidated Holocene deposits and/or non-engineered fill that are too small for the map

scale. A Very Low rating was assigned to Tertiary volcanic rocks (unit Tv) exposed along the margins of the inner Rio Grande valley (Kelson et al., 1999).

3.2 Earthquake Scenario and Probabilistic Ground Motion Maps

Intensities associated with moderate pre-instrumental earthquakes (Olsen, 1979) suggest that peak ground accelerations (PGA) in the middle Rio Grande Valley may have been sufficient to trigger liquefaction in highly susceptible sediments, although no instances of liquefaction or paleoliquefaction have been reported. Earthquake-induced liquefaction can occur over widespread areas during long-duration, strong ground shaking with a PGA equal to or greater than 0.15 g (Tinsley et al., 1985), which may be produced by large-magnitude earthquakes ($M \geq 6.5$).

Within central New Mexico, there are several potential seismic sources that are capable of producing a PGA greater than 0.15 g in metropolitan Albuquerque. These include the Sandia-Rincon fault along the western margin of the Sandia Mountains, the West Mesa fault zone west of the Rio Grande, and the Hubbell Spring fault bordering the Manzanita and Manzano Mountains (Figure 1; Wong et al., 1996; Connell, 1996; Machette et al., 1998).

GIS-based earthquake scenario and probabilistic ground motion maps are available for the Albuquerque-Santa Fe corridor (Wong et al., 2000; 2004). These maps consist of gridded (0.1 km spacing) ground motion values for peak horizontal acceleration and horizontal spectral accelerations at 0.2 and 1.0 sec periods. Existing scenario maps are for a moment magnitude (M_w) 7.0 earthquake on the Sandia-Rincon fault. Probabilistic ground motion estimates are available for the two average return periods of building code relevance: 500 and 2,500 years (Wong et al., 2000; 2004).

Our assessment of liquefaction potential for the Albuquerque area utilizes the approach developed by Youd and Perkins (1978), which emphasizes the merging of liquefaction susceptibility mapping with liquefaction opportunity information. For this project, we digitized the surficial geologic and liquefaction susceptibility maps produced for NEHRP (Kelson et al, 1999). We used these maps, with ground motion maps produced for the Albuquerque-Santa Fe corridor by Wong et al (2000, 2004), to produce liquefaction potential maps, as described below.

Our method of mapping susceptibility to liquefaction includes correlation of the age and type of geologic unit with depth to groundwater and the threshold triggering PGA required for initiation of liquefaction (Hitchcock et al., 1999; Kelson et al., 1999). Keying liquefaction susceptibility ratings to estimated threshold triggering ground motion values allows changes in liquefaction potential for various earthquake scenarios to be assessed across the study area. From our previous geologic mapping (Plate 1) and associated liquefaction susceptibility mapping (Plate 2), each susceptibility map unit (digital polygon) is associated with a threshold ground motion that is predicted to trigger liquefaction (Kelson et al., 1999). Additionally, the liquefaction susceptibility ratings incorporate parameters that may change with time, including depth to groundwater and, therefore, can be modified in the future to reflect new or additional data.

We incorporated the existing probabilistic and scenario ground motion data with our existing liquefaction susceptibility maps to generate liquefaction potential maps (e.g. Figure 3). For the Mw7.0 scenario earthquake on the Sandia-Rincon fault, we digitally compared the ground motions throughout the study area (predicted by Wong et al., 2000) with the susceptibility map unit thresholds, and identified the polygons (or parts of polygons) within which the threshold is exceeded and liquefaction potentially might occur. Similarly, from ground motion values generated by Wong et al. (2000), we compared the predicted ground motion for each of the probability levels with the threshold ground motion calculated for liquefaction susceptibility map units (polygons), to produce maps depicting areas for which the PGA ‘triggering’ threshold is exceeded, and liquefaction potentially may occur.

4.1 Scenario-based Liquefaction Potential Maps

In the scenario-based approach, a specific earthquake is selected (i.e., with a particular magnitude and location) and ground motions are computed using applicable attenuation relations.

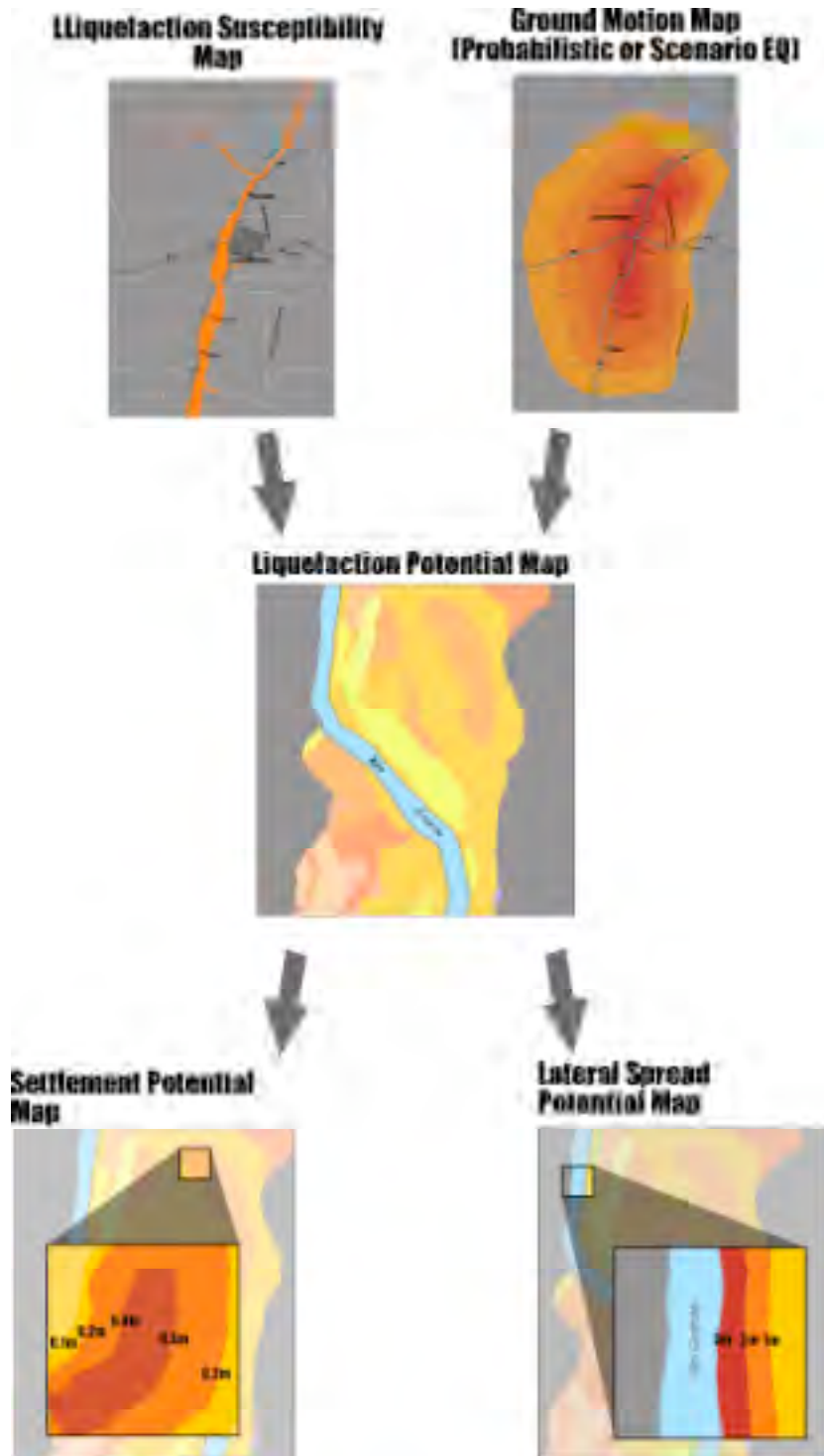


Figure 3. Maps showing integration of existing NEHRP-funded products: liquefaction susceptibility map (Kelson et al, 1999) and, ground motion maps (Wong et al, 2000; 2004) to produce: liquefaction potential, settlement potential, and lateral spread potential maps.

Because our existing liquefaction susceptibility map units incorporate the estimated threshold ground motion values required to initiate liquefaction (e.g. PGA triggering values), the calculation of liquefaction potential for a scenario earthquake with an anticipated magnitude in the range of Mw 7.0 is fairly straightforward. Anticipated ground motions calculated for a scenario earthquake are directly compared to the threshold, or “triggering”, values associated with liquefaction susceptibility to calculate liquefaction potential. The resultant deterministic liquefaction potential map depicts the areas of possible liquefaction for a large earthquake.

Earthquake-induced liquefaction can occur within susceptible sediments over widespread areas during long-duration, strong ground shaking with a peak ground surface acceleration (PGA) value equal to or greater than 0.15 g (Tinsley et al., 1985). Analyses of strong ground motions in the region suggest that rupture along the Sandia-Rincon fault may produce PGA values exceeding 0.8 g (Wong et al., 2000; 2004).

Input files used in producing the liquefaction potential map for a large earthquake on the Sandia-Rincon fault included: (1) our previously completed liquefaction susceptibility map units (Kelson et al., 1999) and, (2) PGA values from a M7.0 event on the Sandia-Rincon fault calculated by Wong et al (2004). Before directly comparing the scenario-based PGA values to the triggering PGA values associated with the liquefaction susceptibility map units, we added a new descriptive database field to the liquefaction susceptibility map database. This database field provides estimated triggering PGA for each map unit within the existing database. This information is derived from our original liquefaction susceptibility mapping (Kelson et al., 1999). The PGA trigger values, derived from the analyses performed for our previous mapping of liquefaction susceptibility, are provided below:

<u>Susceptibility</u>	<u>PGA trigger</u>
very high	.1
high	.2
medium	.3
low	.4
very low	.5 or greater

In order to calculate the final liquefaction potential map, we intersected the polygons within the scenario-based ground-motion map layer with the polygons within the liquefaction susceptibility map layer. The intersected map layer has an associated merged database with fields for the

estimated triggering PGA, with the categories listed above derived from the susceptibility map layer, and the calculated PGA value, derived from the buffered ground motions calculated from the scenario earthquake on the Sandia-Rincon fault. We then subtracted the triggering PGA field value, derived from the susceptibility map layer, from the anticipated PGA field, derived from the ground-motion map layer, to create an output numeric field termed “PGA exceedance”. This field consists of the amount that predicted ground motion exceeds the threshold ground motion required for initiation of liquefaction. We then qualitatively assigned the following probability of liquefaction values based on the calculated PGA exceedance value:

<u>PGA exceedance</u>	<u>Probability of liquefaction</u>
0.4 g or greater	very high
0.2 to 0.4 g	high
0 to 0.2 g	moderate

Our final map (Plate 3) thus fully incorporates the calculated values for initiation (‘triggering’) of liquefaction within saturated, liquefiable deposits based on the properties of the mapped deposits. Unsaturated Quaternary geologic units and areas underlain by young deposits with calculated ground motions that do not match or exceed calculated triggering PGA values are assigned a “low” classification. Bedrock within the final map liquefaction potential map layer is classified as having a “very low” potential for liquefaction.

4.2 Probabilistic-based Liquefaction Potential Maps

Similar to the deterministic approach used to map liquefaction potential for a scenario event on the Sandia-Rincon fault, the probabilistic-based liquefaction potential map of the inner Rio Grande Valley was generated through digital integration of multiple data sets. However, in the probabilistic approach, consideration of multiple potential earthquake sources yields the annual probability that a given level of ground motion will be exceeded at each location of interest in the study area. To facilitate liquefaction analysis, hazard deaggregation is required to determine the modal, or most likely, earthquake magnitude that can be paired with each spatially unique ground-motion estimate to calculate liquefaction potential.

The potential for liquefaction is dependent upon the opportunity for ground motions to exceed the threshold level required for initiation of liquefaction. We incorporated probabilistic ground motion estimates available for the two average return periods of building code relevance: 500 and 2,500 years. Production of the probabilistic liquefaction potential map of Albuquerque required digital comparison of peak ground surface accelerations (PGA values) with a 10% probability of

exceedance over a 50-year period (500-year return period) against the threshold ground motions required to initiate liquefaction in different geologic deposits across the region (Plate 4). Similarly, we evaluated the potential for liquefaction given PGA values with a 2% probability of exceedance over a 50-year period (2,500 year return period) (Plate 5). By overlying and querying these distinct data sets within GIS, we have identified and characterized areas where ground motions may exceed the threshold levels required for liquefaction within the period of interest.

Similar to the final map production for the scenario-based liquefaction potential map, we intersected the polygons within the probabilistic ground-motion map layer with the polygons within the liquefaction susceptibility map layer. We obtained a merged database with fields for the estimated triggering PGA, with the categories listed above derived from the susceptibility map layer, and the calculated PGA value, derived from the probabilistic ground motions. We then subtracted the triggering PGA field value, derived from the susceptibility map layer, from the anticipated PGA field, derived from the ground-motion map layer, to create an output numeric field termed “PGA exceedance”. Finally, we characterized those map unit polygons (or parts of polygons) for which the liquefaction threshold is exceeded and classified the potential for liquefaction based on the amount that the threshold PGA value is exceeded. It is this value, based on the same classification as that used in the Sandia-Rincon scenario-based liquefaction potential map, that we then used as our legend for our final map layer.

Because modal earthquake magnitudes associated with ground-motion estimates vary spatially across the study area, the quantitative liquefaction analyses required to accurately evaluate liquefaction potential need to be corrected or ‘scaled’ for magnitude. This correction is necessary because a given peak acceleration at a specific location produced by a nearby small earthquake typically is not as damaging as the same acceleration produced by a more distant large earthquake. The reason for the difference is that the larger magnitude earthquake produces more cycles of strong ground motion than does the smaller magnitude event, even though both may produce the same peak acceleration.

For example, during the Mw 6.8 1994 Northridge earthquake, mapped areas with high to very high liquefaction susceptibility that experienced ground shaking greater than the calculated threshold ground motions required to initiate liquefaction in an ‘average’ earthquake of Mw 7.5 did not exhibit surface evidence of liquefaction. In part, the failure to liquefy likely is because liquefaction susceptibility mapping of Simi Valley (Hitchcock et al., 1999), and our regional liquefaction susceptibility mapping, is based on the 15 strain cycles associated with a ‘standard’ Mw 7.5

earthquake. A seismograph (USC Station #55) at the Knolls Elementary School in Simi Valley recorded 12 to 13 strain cycles (Adel-Haq and Hryciw, 1998).

It is therefore likely that a higher threshold ground motion value is required to initiate liquefaction to compensate for a lower number of loading cycles associated with a smaller magnitude earthquake. The number of strain cycles that a deposit undergoes directly influences the likelihood of liquefaction occurring in a deposit. Variation in earthquake magnitude, i.e. variation in number of strain cycles, changes the minimum ‘triggering’ ground motion required to initiate liquefaction. Essentially, liquefaction analyses of individual borings used in determining regional liquefaction susceptibility need to be recalculated to incorporate a magnitude correction or ‘scaling’ factor. These analyses are necessary to obtain the magnitude dependent ‘triggering’ PGA values required to initiate liquefaction in near-surface, saturated deposits during different earthquake sources.

Permanent ground deformation (PGD) triggered by liquefaction, in particular lateral spreading, is one of the primary causes of damage during large earthquakes. Recent examples of liquefaction-related ground deformation include large-scale damage produced during the 1989 Loma Prieta, 1994 Northridge, 1995 Kobe, 1999 Turkey, and 2001 Indian earthquakes. These, and other historical earthquakes, show that the thickness, depth, slope, and lateral continuity of buried liquefiable units, and their intersection with streambanks and other free faces, directly controls the distribution of liquefaction-related ground failure during large earthquakes.

Mapping the three-dimensional distribution of liquefaction hazard is required for accurate depiction of possible ground deformation during an earthquake. This, in turn, requires correlation of mapped, susceptible surficial deposits to potentially liquefiable sediments beneath the valley floor. The thickness, depth, slope, and lateral continuity of buried liquefiable units, and their intersection with streambanks, drainage ditches, flood-control levees, and other free faces, typically control the distribution of lateral spreads during large earthquakes (Bartlett and Youd, 1992).

Potential ground settlement and lateral spread maps were constructed at a scale of 1:24,000, for a portion of the Albuquerque West quadrangle, which covers downtown Albuquerque and contains several locations where subsurface data are adequate for quantifying the potential amounts of ground deformation. The three-dimensional liquefaction hazard mapping involved the following tasks:

- (a) Construction of maps of thickness of liquefiable deposits;
- (b) Construction of liquefaction-induced settlement maps; and
- (c) Construction of potential lateral spread maps.

The current borehole database, compiled in cooperation with the NMBGMR (Clark and Haneberg, 2001, 2004; Clark, 2003), although comprehensive, is not sufficient to fully characterize the subsurface geometry and composition of susceptible geologic units. Borehole data were not evenly distributed across the study area. Therefore interpolation of data across the entire study area by Clark (2003) using geostatistical methods was incorporated in our analyses.

5.1 Ground Settlement

We used isopach maps of liquefiable sediments, calculated using historic groundwater depths, to derive conservative estimates of the magnitude of liquefaction-induced settlement. We estimate the

amounts of potential liquefaction-induced settlement from empirical relations given by Tokimatsu et al. (1987) and Glaser (1993, 1994). We estimate the amounts of potential liquefaction-induced settlement from empirical relations given by Tokimatsu and Seed (1987), Ishihara and Yoshimine (1992), and Glaser (1993, 1994). These methods have been developed to predict the magnitude of liquefaction-induced settlement in sandy deposits during the scenario earthquake. Typically, application of these techniques to areas with well-sorted (poorly graded) sand yields volumetric strains of 1 to 5 percent. We have incorporated an isopach maps, showing the thickness of liquefiable sediments, to derive conservative estimates of the magnitude of possible liquefaction-induced settlement (Figure 4).

Because of uncertainties inherent in these empirical relationships, our maps show the maximum potential settlement, based on the borehole data for each mapped geologic unit. For example, for deposits with only moderate susceptibility to liquefaction, we multiply the thickness of liquefiable materials by 1-2 percent, whereas for highly susceptible deposits we multiply the thickness of the deposit by 5-6 percent, to obtain a conservative estimate of the possible volumetric strain.

5.2 Lateral Spread

Lateral spreading is permanent ground deformation caused by the horizontal movement of overlying sediments on a laterally continuous, liquefied layer towards a free face (e.g., stream channel or cut bank) or on a slope. Lateral spreading poses one of the greatest liquefaction-induced, ground-deformation hazards to engineered structures, including buildings, critical facilities, and lifelines.

Our existing two-dimensional liquefaction susceptibility maps, and susceptibility isopach mapping form the framework for predicting the extent and magnitude of lateral displacements. Factors that we considered in estimating the amount of lateral displacement include: (1) the thickness of unconsolidated sediment subject to liquefaction, (2) duration and peak ground acceleration of ground shaking, (3) slope, and (4) height and distance from a free face, and whether the liquefiable layer intersects the free face. We utilize empirical relations and procedures presented by Bartlett and Youd (1992, 1997), Glaser (1993, 1994), Bardet et al (1999), and Youd et al. (1999) to calculate lateral spread displacements.

We use existing 10-m digital elevation model (DEM) and LiDAR data to identify and characterize free-face slopes. The derived slope data is used, in conjunction with the existing geologic data and the available geotechnical database, to identify the susceptibility of geologic units to lateral

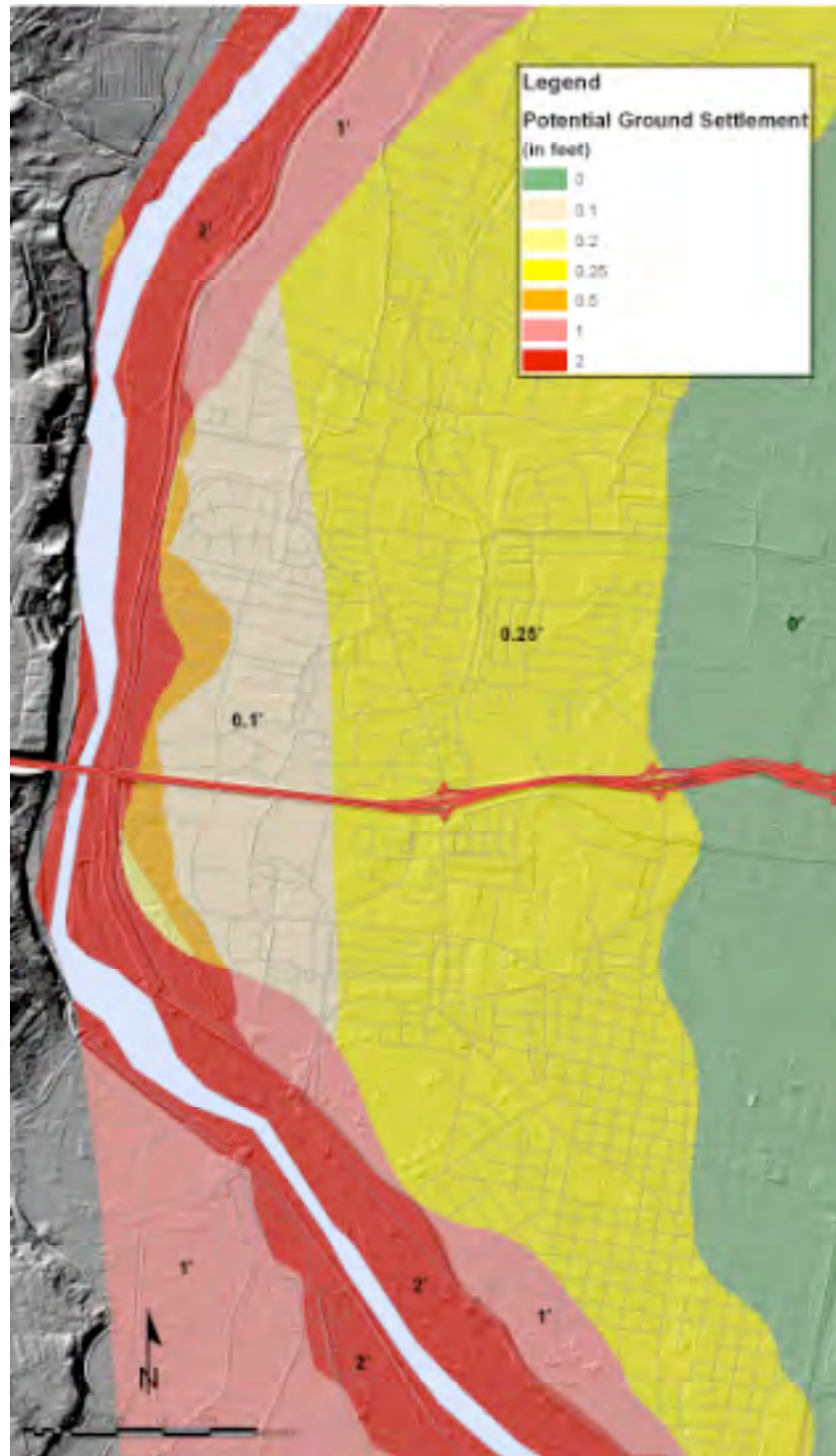


Figure 4. General map of downtown Albuquerque area showing settlement potential, based on fines content and thickness of saturated sediments on LiDAR base map.

spreading based on the distance from the free-face of likely spreading and estimated magnitude of displacement.

Bartlett and Youd (1992, 1995, 1997) developed an empirical model on the basis of multiple linear regression (MLR) analyses for predicting the horizontal ground displacement resulting from liquefaction-induced lateral spread based on data from Japanese and U.S. earthquakes. Based on the examination of various parameters through statistical means, Bartlett and Youd (1992) identified the following parameters as controlling parameters of liquefaction induced ground deformation:

D horizontal displacement (m)

M_w moment magnitude

R nearest horizontal distance (km) to seismic energy source or fault rupture

S slope (%) of ground surface

W free face ratio (%)

T₁₅ thickness (m) of saturated cohesionless soils (excluding depth >20 and >15% clay content) with N₁₆₀<15

F₁₅ average fine content (% finer than 75 μm)

D₅₀₁₅ average D₅₀ grain size (mm) in T₁₅

Bardet et al. (1999) incorporated the Bartlett and Youd (1995) database and have proposed a four-parameter MLR model of the form:

$$\begin{aligned} \text{Log} (D + 0.01) = & b_0 + b_{\text{off}} + b_1 M_w + b_2 \text{Log} (R) + b_3 R \\ & + b_4 \text{Log} (W) + b_5 \text{Log} (S) + b_6 \text{Log} (T_{15}) \end{aligned}$$

where the b-coefficients are derived from MLR analyses, and are summarized by Bardet et al. (1999). In free-face cases, the term Log (S) is zero. In ground slope cases, the term Log (W) is zero.

We map lateral spreads using the empirical approach refined by Bardet et al. (1999) because it incorporates updates of the Bartlett and Youd database and reduces inherent errors due to the narrow value range of some parameters (e.g., F₁₅, and D₅₀₁₅; Bardet et al., 1999).

Because the various empirical relations require values for earthquake magnitude and epicentral distance, we incorporate the scenario earthquake to estimate lateral spread displacements.

We acknowledge that in some highly susceptible areas of liquefaction, lateral spreading may occur in the down-slope direction without the presence of a free-face. However, these areas are highly difficult to identify. Pease and O'Rourke (1998) showed a strong correlation, independent of free faces, between maximum lateral displacements observed in the 1906 San Francisco earthquake and the mapped thickness of underlying saturated fill. We therefore believe that areas of potential lateral spread in the absence of a free face likely will be confined within portions of the inner Rio Grande Valley with thick saturated fill. Thus, our isopach maps of liquefiable sediments may highlight areas that will experience localized lateral spreading missed using proposed empirical approach.

Our analysis of the Albuquerque area suggests that nearly all of the sediments in the inner valley could experience localized initiation of liquefaction, where saturated, and possible ground failure given the occurrence of a large ($M=7.0$) earthquake on the Sandia-Rincon fault near Albuquerque (Plate 3). PGA values required for initiation of liquefaction are exceeded throughout much of the central valley, including the western portion of downtown Albuquerque. However, the potential for liquefaction is greatest north of Albuquerque in the Bernallilo and Corrales areas, with the greatest hazard localized within the narrow Rio Grande valley, adjacent to the river. In part this is a natural result of the presence of saturated, poorly consolidated deposits along the river course. However, the potential for liquefaction also likely is directly correlative to the proximity of this area to the Sandia-Rincon fault.

Derivation of liquefaction potential from probabilistic ground motion estimates available for the two average return periods of building code relevance, 500 and 2,500 years, suggests that widespread liquefaction is possible within both time periods. Comparison of peak ground surface accelerations (PGA values) with a 10% probability of exceedance over a 50-year period (500-year return period) against the threshold ground motions required to initiate liquefaction in different geologic deposits across the region (Plate 4), shows a moderate to high potential for liquefaction, with the highest potential in the Bernallilo area, north of Albuquerque. The potential for liquefaction given PGA values with a 2% probability of exceedance over a 50-year period (2,500 year return period) is greater throughout the inner valley, but still greatest north of Albuquerque (Plate 5).

We have integrated our existing NEHRP-funded liquefaction susceptibility maps (Kelson et al., 1999) with NEHRP-funded ground motion potential maps (Wong et al, 2004) to prepare liquefaction potential maps. For this project, we digitized the surficial geologic and liquefaction susceptibility maps produced for NEHRP by Kelson et al. (1999). We used these maps, with ground motion maps produced for the Albuquerque-Santa Fe corridor by Wong et al (2000, 2004), to produce liquefaction potential maps. The maps depict the potential for liquefaction for a possible Mw7.0 earthquake on the Sandia-Rincon fault and for 500- and 2,500-year return periods. Because of the relatively low rate of historic seismicity in the Rio Grande rift, the liquefaction potential maps presented in this report likely more accurately depict the distribution and likely severity of liquefaction hazard in the Albuquerque metropolitan region than the liquefaction susceptibility maps.

Based on our previous synthesis of the geologic, geotechnical, and groundwater data, (Kelson et al., 1999), large areas of the inner Rio Grande valley are susceptible to liquefaction. Overall, the areas classified as having a Very High or High liquefaction susceptibility include most of the inner Rio Grande valley. This area involves roughly 240 square kilometers (90 square miles) within the valley north and south of Albuquerque. However, the potential for liquefaction from either a scenario earthquake on the Sandia-Rincon fault or all sources over a 500 to 2,500 year period, is greatest north of Albuquerque. The highest potential for ground failure likely is in the Bernallilo and Corrales areas, localized within the narrow Rio Grande valley, adjacent to the river. Overall, it is reasonable to assume that areas of the inner valley along the river within downtown Albuquerque and north may be affected by localized liquefaction-related ground failure. Lateral spreads likely will be heavily influenced by the presence of natural and man-made river banks. Localized ground settlement likely will be controlled by the subsurface distribution of river sands within abandoned river channels adjacent to the current Rio Grande.

Many people helped us collect geotechnical and groundwater data during the course of this study. We are most grateful to Jodi Clark of New Mexico Tech for graciously providing in-progress data and collaborating with us on the project. Thanks especially to Laura Bexfield and Doug McAda of the U.S. Geological Survey, Water Resources Division, and to Steve Jetter and Bart Faris of the State of New Mexico Environmental Department. Thanks also to Jeffrey Peterson of the Bernalillo County Environmental Health Department, Steve Hanson of the U.S. Bureau of Reclamation, Janet Slate and Steve Personius of the U.S. Geological Survey, Mic Heynekamp and Dave Love of the New Mexico Bureau of Mines and Mineral Resources, John Stomp of the City of Albuquerque Public Works Department, John Kelly of the Albuquerque Metropolitan Arroyo Flood Control.

- Adel-Haq, A and R. D. Hryciw, 1998, Ground settlement in Simi Valley following the Northridge earthquake, *Journal of Geotechnical and Geoenvironmental Engineering*, vol. 124, no.1 pp. 80-89.
- Bardet, J. P., N. Mace, T. Tobita, and J. Hu, 1999, Large-Scale Modeling of Liquefaction-Induced Ground Deformation Part I: A Four-Parameter MLR Model, *Technical Report MCEER-99-0019*, Multidisciplinary Center for Earthquake Engineering Research, State University of New York at Buffalo, Buffalo, NY, 1999a, 155-173.
- Bartlett, S.F., and Youd, T.L., 1992, Empirical prediction of lateral spread displacement: National Center for Earthquake Engineering Research Technical Report 92-0019, p. 351-366.
- Bartlett, S. F. and T. L. Youd, 1995, Empirical Prediction of Liquefaction-Induced Lateral Spreading, *Journal of Geotechnical Engineering*, ASCE, Vol. 121, No. 4, 316-329.
- Clark, J.A. and Haneberg, W.C., 2001, Engineering geologic and liquefaction susceptibility analysis of the Inner Valley, Rio Grande Basin, Albuquerque, New Mexico: GSA 2001 Rocky Mountain/South-Central Section Meeting Abstracts with Programs.
- Clark, J.A.. 2003, Liquefaction susceptibility mapping of the shallow alluvium, Inner Valley, Rio Grande Basin, Albuquerque, New Mexico. M.S. in Geology, NM Tech.
- Clark, J.A. and Haneberg, W.C., 2004, GIS based methods for three-dimensional evaluation of liquefaction susceptibility, Albuquerque, NM: Geological Society of America Abstracts with Programs, v.36, p. 298.
- Connell, S.D., 1997 (last revised: 2 Feb 2000), Geology of the Alameda 7.5' quadrangle, Bernalillo and Sandoval Counties, New Mexico, New Mexico Bureau of Mines and Mineral Resources, Open-file Geologic Map OF-GM 10, scale 1:24,000.
- Connell, S.D., Allen, B.D., Hawley, J. and Shroba, R., 1998 (last revised: 4 Feb 2000), Geology of the Albuquerque West 7.5-min. quadrangle, Bernalillo County, New Mexico, New Mexico Bureau of Mines and Mineral Resources, Open-file Geologic Map OF-GM 17, scale 1:24,000.
- Connell, S.D., Cather, S.M., Ilg, B., Karlstrom, K.E., Menne, B., Picha, M., Andronicos, C., Read, A.S., Ilg, B., Bauer, P.W., Johnson, P.S., 1995 (last revised: 17 Feb 2000), Geology of the Bernalillo and Placitas 7.5-min quadrangles, Sandoval County, New Mexico: New Mexico Bureau of Mines and Mineral Resources, Open-file Geologic Map OF-GM 2 and 16, scale 1:24,000. (mapped at 1:12,000).
- Connell, S.D., 1997, Geology of the Alameda 7.5-minute quadrangle, Bernalillo and Sandoval Counties, New Mexico: New Mexico Bureau of Mines and Mineral Resources Open-file Digital Map OF-DM 10, scale 1:24,000; printed August 25, 1998.
- Connell, S.D., 1998a, Preliminary geologic map of the Albuquerque West 7.5-minute quadrangle, Bernalillo County, New Mexico: New Mexico Bureau of Mines and Mineral Resources Open-file Digital Map OF-DM 17, scale 1:24,000; dated October 28, 1998.
- Connell, S.D., 1998b, Preliminary geologic map of the Bernalillo 7.5-minute quadrangle, Sandoval County, New Mexico: New Mexico Bureau of Mines and Mineral Resources Open-file Digital Map OF-DM 16, scale 1:24,000; printed August 27, 1998.
- Chen, A.T., 1988, PETAL3: Penetration testing and liquefaction, An interactive computer program: U.S. Geological Survey Open-file Report 88-540, 34 p.
- Clark, J.D., 2004, Liquefaction susceptibility mapping of the shallow alluvium, Inner Valley, Rio Grande Basin, Albuquerque, New Mexico. M.S. in Geology, NM Tech.
- Clark, J.A. and Haneberg, W.C., 2001, Engineering geologic and liquefaction susceptibility analysis of the Inner Valley, Rio Grande Basin, Albuquerque, New Mexico: GSA 2001 Rocky Mountain/South-Central Section Meeting Abstracts with Programs.
- Glaser, S., 1993, Estimating in situ liquefaction potential and permanent ground displacements due to liquefaction for the siting of lifelines: National Institute of Standards and Technology Report NISTIR 5150, 103 p.

- Glaser, S.D., 1994, Estimation of surface displacements due to earthquake excitation of saturated sands: *Earthquake Spectra*, Vol. 10, No. 3, p. 489-517.
- GRAM/William Lettis & Associates, Inc., 1995, Conceptual geologic model of the Sandia National Laboratories and Kirtland Air Force Base: unpublished consultant's report to Environmental Restoration Project, Sandia National Laboratories, 3 volumes.
- Grant, P.W. and Perkins, W.J., 1994, Liquefaction hazard evaluation, Seattle, Washington: Proceedings Fifth U.S. National Conference on Earthquake Engineering, Chicago Illinois, Vol. IV, p. 127-135.
- Hawley, J.W., and Haase, C.S., 1992, Hydrogeologic framework of the northern Albuquerque basin: New Mexico Bureau of Mines and Mineral Resources Open-file Report 387, 165 p.
- Hitchcock, C.S., Loyd, R.C., and Haydon, W.D., 1996, Liquefaction susceptibility and hazard zone mapping, Simi Valley, California [abs.], *Eos*, V. 77, no. 46, p. F510.
- Idriss, I.M., 1997, Evaluation of liquefaction potential and consequences: Seismic Short Course on Evaluation and Mitigation of Earthquake Induced Liquefaction Hazards, NCEER Workshop, San Francisco, CA, March, 1997.
- Johnson, N.M., and Dreiss, S.J., 1989, Hydrostratigraphic interpretation using indicator geostatistics: *Water Resources Research*, v. 25, p. 2501-2510.
- Jones, C.F., Youd, T.L., and Mabey, M.A., 1994, Liquefaction hazard maps for the Portland, Oregon quadrangle: Proceedings, Fifth U.S. National Conference on Earthquake Engineering, Earthquake Engineering Research Institute, v. 4, p. 209-218.
- Kelson, K.I., Hitchcock, C.S., and Randolph, C.E., 2001, Surface geology and liquefaction susceptibility mapping in the Middle Rio Grande Basin, Albuquerque, New Mexico: New Mexico Bureau of Geology and Mineral Resources Open-file Report 454C and 454D, p. B-1 to B-5.
- Kelson, K.I., Hitchcock, C.S., and Randolph, C.E., 2001, Liquefaction susceptibility mapping in the metropolitan Albuquerque region, New Mexico: [abs] *Geological Society of America abstracts with programs*, Vol. 33, no.5, p. A-49.
- Kelson K.I., Hitchcock, C.S., Sawyer, T.L., Thomas, E.C., and Gibson, J.D., 1994, Reducing uncertainty in assessment of the hydrogeologic framework: Characterization of surficial deposits at Sandia National Laboratory, New Mexico: [abs.]: *Eos*, v. 75, no. 44, p. 278.
- Kelson, K.I., Hitchcock, C.S., and Randolph, C.E., 1999, Liquefaction susceptibility in the Inner Rio Grande Valley near Albuquerque, New Mexico: Final Technical Report, U.S. Geological Survey, Award 98-HQ-GR-1009, 40 p. + appendices.
- Law, K.T., Cao, Y.L., and He, G.N., 1985, An energy approach for assessing seismic liquefaction potential: *Canadian Geotechnical Journal*, v. 27, p. 320-329.
- Makdisi, F. I., and Seed, H. B., "Simplified Procedure for Estimating Dam and Embankment Earthquake - Induced Deformations", *Journal of the Geotechnical Engineering Division, ASCE*, Vol. 104, No. GT7, July 1978.
- Machette, M.N., and McGimsey, R.G., 1982, Quaternary and Pliocene faults in the Socorro and western part of the Fort Sumner 1° x 2° quadrangles, New Mexico: U.S. Geological Survey Miscellaneous Field Studies Map MF-1465-A, scale 1:250,000.
- Machette, M.N., Personius, S.F., Kelson, K.I., and Seager, W.R., 1996, New digital map and computer database of Quaternary faults and folds in New Mexico: *Geological Society of America Abstracts with Program*, v. 28, no. 7, p. A-377.
- Machette, M.N., Personius, S.F., Kelson, K. I., Dart, R.L., and Haller, K.M., 1998, Map and data for Quaternary faults in New Mexico: USGS Open-file Report 98-521, 443 pp.
- Newmark, N. M., 1965, "Effects of Earthquakes on Embankments and Dams," *Géotechnique*, 15, No.2, pp.139-160.
- Olsen, K.H., 1979, The seismicity of north-central New Mexico with particular reference to the Cerrillos earthquake of May 28, 1918: *New Mexico Geological Society Guidebook* 30, p. 65-75.
- Personius, S.F., Machette, M.N., and Kelson, K.I., 1999, Quaternary faults in the Albuquerque area-- An update: *New Mexico Geological Society Guidebook* 50, p. 189-200.

- Personius, S.F., Eppes, M.C., Mahan, S.A., Love, D.W., Mitchell, D.K., and Murphy, A., 2001, Log and data from a trench across the Hubbell Spring fault zone, Bernalillo County, New Mexico: U.S. Geological Survey Miscellaneous Field Studies Map MF-2348, v. 1.1.
- Robertson, P.K., and Wride, C.E., 1997, Cyclic liquefaction and its evaluation based on SPT and CPT: Seismic Short Course on Evaluation and Mitigation of Earthquake Induced Liquefaction Hazards, NCEER Workshop, San Francisco, CA, March, 1997.
- Sandia National Laboratories, 1994, Site Wide Hydrogeologic Characterization Project, Calendar Year 1993 Annual Report: unpublished report, Sandia National Laboratory, Albuquerque, New Mexico, variously paginated.
- Seed, H.B., and Idriss, I.M., 1971, Simplified procedure for evaluating soil liquefaction potential: Proceeding of the American Society of Civil Engineers, Journal of the Soil Mechanics and Foundations Division, v. 93, no. SM9, p. 1249-1273.
- Seed, H.B., and Idriss, I.M., 1982, Ground motions and soil liquefaction during earthquakes: Earthquake Engineering Research Institute, Engineering Monograph volume 5, 134 p.
- Seed, H.B., Idriss, I.M., and Arango, I., 1983, Evaluation of liquefaction potential using field performance data: American Society of Civil Engineers, Journal of Geotechnical Engineering, v. 109, no. 3, p. 458-482.
- Seed, H. B., Tokimatsu, K., Harder, L. F., and Chung, R. M., 1985, Influence of SPT procedures in soil liquefaction resistance evaluations: Journal of Geotechnical Engineering, ASCE, vol. 111, no. 12, pp. 1425-1445.
- Seed, R. B., and Harder, L.F., 1990, SPT-based analysis of cyclic pore pressure generation and undrained residual strength, *in* Duncan, M.J., editor, H. Bolton Seed Memorial Symposium Proceedings, May, 1990: BiTech Publishers, Vancouver, B.C., Canada, p. 351-376.
- Tinsley, J.C., Youd, T.L., Perkins, D.M., and Chen, A.T.F., 1985, Evaluating Liquefaction Potential, *in* Ziony, J.I., ed., Evaluating earthquake hazards in the Los Angeles Region - an earth-science perspective: United States Geological Survey Professional Paper 1360, p. 263-316.
- Tokimatsu, K., and Seed, H.B., 1987, Evaluation of settlement of sands due to earthquake shaking: Journal of the Geotechnical Engineering Division, ASCE, v. 113, p. 861-878.
- Wong, I.G., Kelson, K.I., and 8 others, 1996, Earthquake potential and ground shaking hazard at the Los Alamos National Laboratory, New Mexico: New Mexico Geological Society Guidebook 47, p. 135-142.
- Wong, Ivan, Olig, Susan, Dober, Mark, Silva Walter, Wright, Douglas, Thomas, Patricia, Gregor, Nick, Sanford, Allan, Lin, Kuo-Wan, Love, David, and Naugler, Wendy, 2000, A new generation of earthquake ground shaking hazard maps for three urban areas in the western U.S.: Part II Albuquerque-Belen-Santa Fe New Mexico corridor [abs]: Proceedings of the 6th International Conference on Seismic Zonation, Palm Springs, CA.
- Wong, Ivan, Olig, Susan, Dober, Mark, Silva Walter, Wright, Douglas, Thomas, Patricia, Gregor, Nick, Sanford, Lin, Kuo-Wan, and David Love, 2004, Earthquake scenario and probabilistic ground-shaking hazard maps for the Albuquerque-Belen-Santa Fe, New Mexico, corridor: New Mexico Geology, v. 26, no.1
- Youd, T.L., 1997, Updates on the simplified procedure: An overview of NCEER workshop in Salt Lake City on liquefaction resistance of soils: Seismic Short Course on Evaluation and Mitigation of Earthquake Induced Liquefaction Hazards, NCEER Workshop, San Francisco, CA, March, 1997.
- Youd, T.L., and Perkins, J.B., 1987, Map showing liquefaction susceptibility of San Mateo County, California: United States Geological Survey, Map I-1257-G.

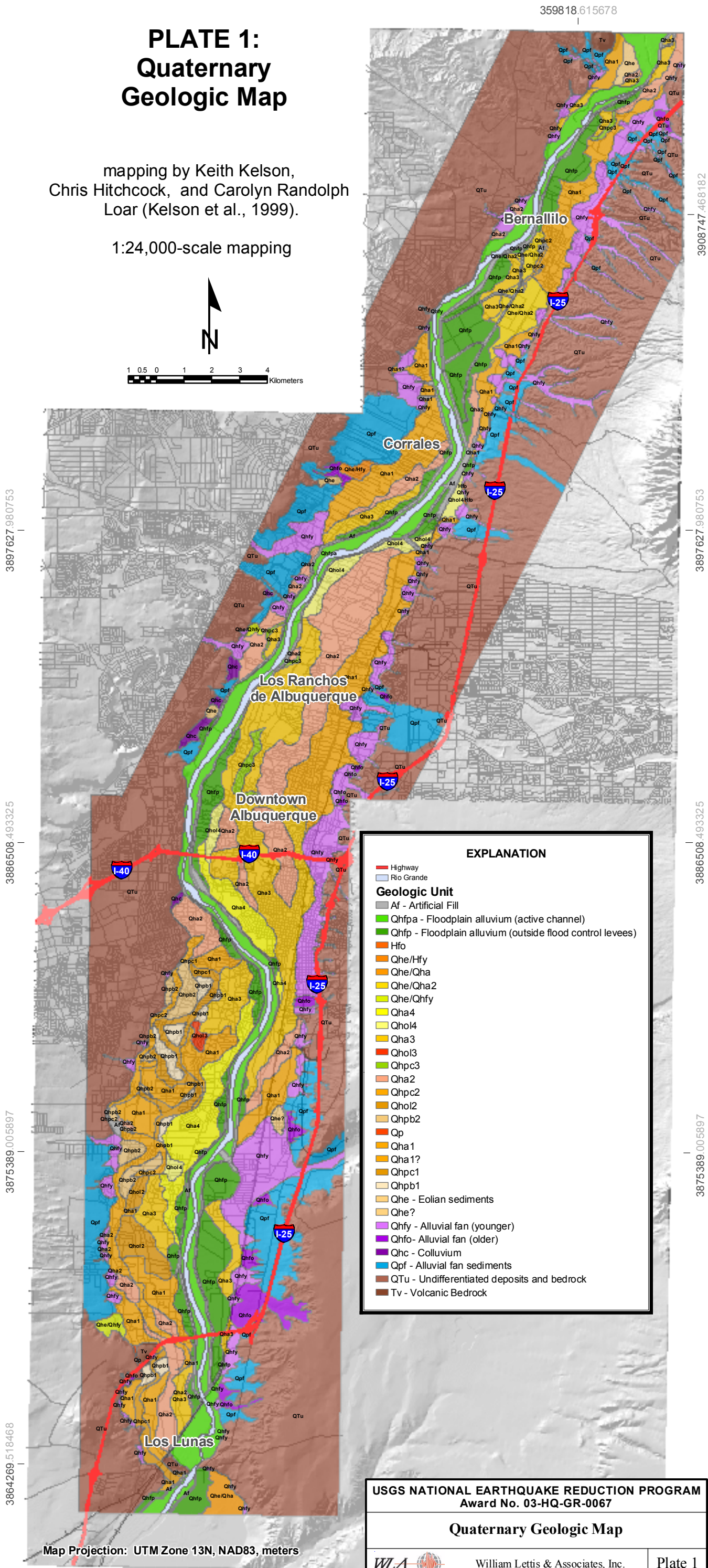
PLATE 1: Quaternary Geologic Map

mapping by Keith Kelson,
Chris Hitchcock, and Carolyn Randolph
Loar (Kelson et al., 1999).

1:24,000-scale mapping



1 0.5 0 1 2 3 4
Kilometers



EXPLANATION

- Highway
- Rio Grande
- Geologic Unit**
- Af - Artificial Fill
- Qhfp - Floodplain alluvium (active channel)
- Qhfp - Floodplain alluvium (outside flood control levees)
- Hfo
- Qhe/Hfy
- Qhe/Qha
- Qhe/Qha2
- Qha4
- Qhol4
- Qha3
- Qhol3
- Qhpc3
- Qha2
- Qhpc2
- Qhol2
- Qhpb2
- Qp
- Qha1
- Qha1?
- Qhpc1
- Qhpb1
- Qhe - Eolian sediments
- Qhe?
- Qhfy - Alluvial fan (younger)
- Qhfo - Alluvial fan (older)
- Qhc - Colluvium
- Qpf - Alluvial fan sediments
- QTu - Undifferentiated deposits and bedrock
- Tv - Volcanic Bedrock

USGS NATIONAL EARTHQUAKE REDUCTION PROGRAM
Award No. 03-HQ-GR-0067

Quaternary Geologic Map



William Lettis & Associates, Inc.

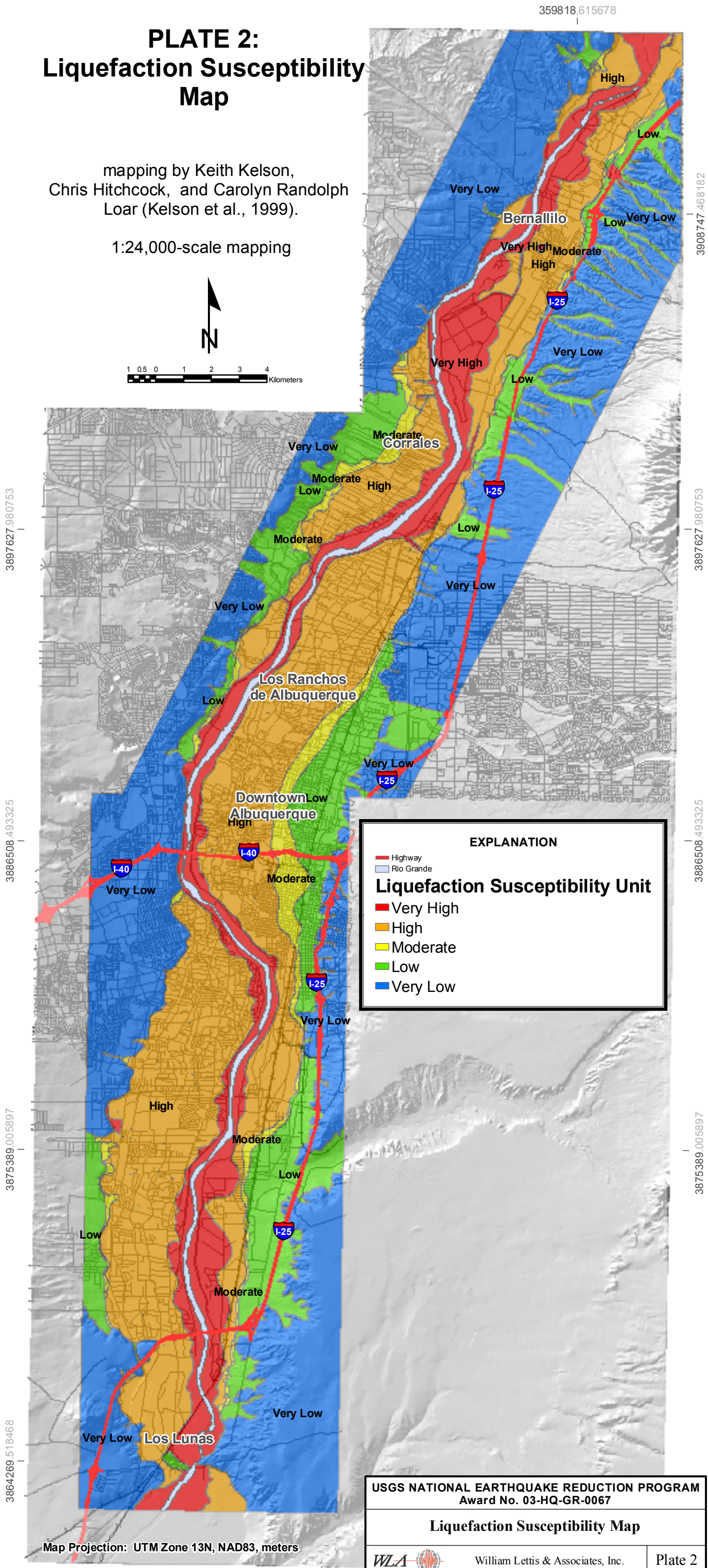
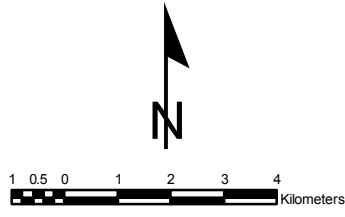
Plate 1

Map Projection: UTM Zone 13N, NAD83, meters

PLATE 2: Liquefaction Susceptibility Map

mapping by Keith Kelson,
Chris Hitchcock, and Carolyn Randolph
Loar (Kelson et al., 1999).

1:24,000-scale mapping



EXPLANATION

- Highway
- Rio Grande

Liquefaction Susceptibility Unit

- Very High
- High
- Moderate
- Low
- Very Low

USGS NATIONAL EARTHQUAKE REDUCTION PROGRAM
Award No. 03-HQ-GR-0067

Liquefaction Susceptibility Map

Map Projection: UTM Zone 13N, NAD83, meters



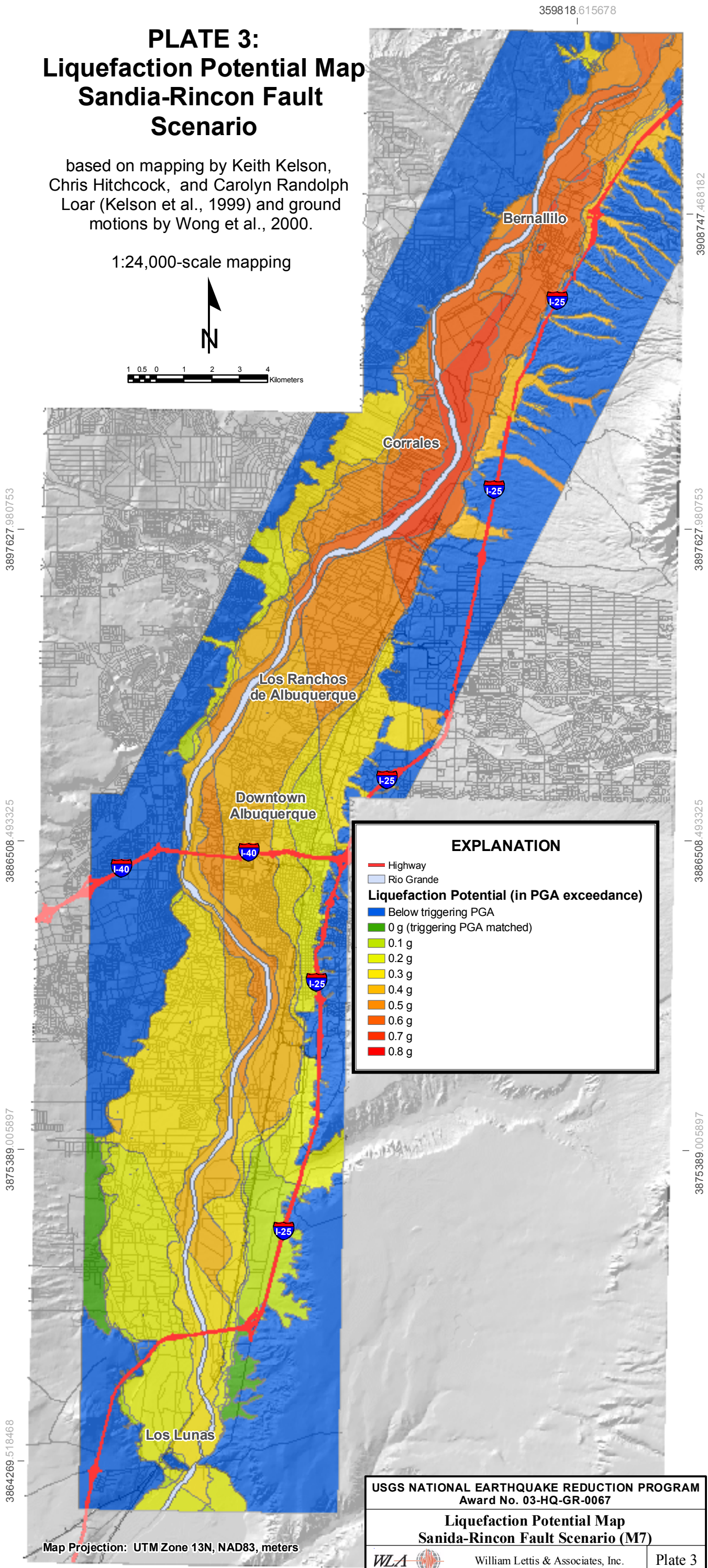
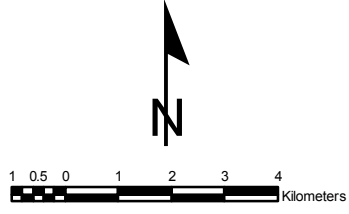
William Lettis & Associates, Inc.

Plate 2

PLATE 3: Liquefaction Potential Map Sandia-Rincon Fault Scenario

based on mapping by Keith Kelson,
Chris Hitchcock, and Carolyn Randolph
Loar (Kelson et al., 1999) and ground
motions by Wong et al., 2000.

1:24,000-scale mapping



EXPLANATION	
	Highway
	Rio Grande
Liquefaction Potential (in PGA exceedance)	
	Below triggering PGA
	0 g (triggering PGA matched)
	0.1 g
	0.2 g
	0.3 g
	0.4 g
	0.5 g
	0.6 g
	0.7 g
	0.8 g

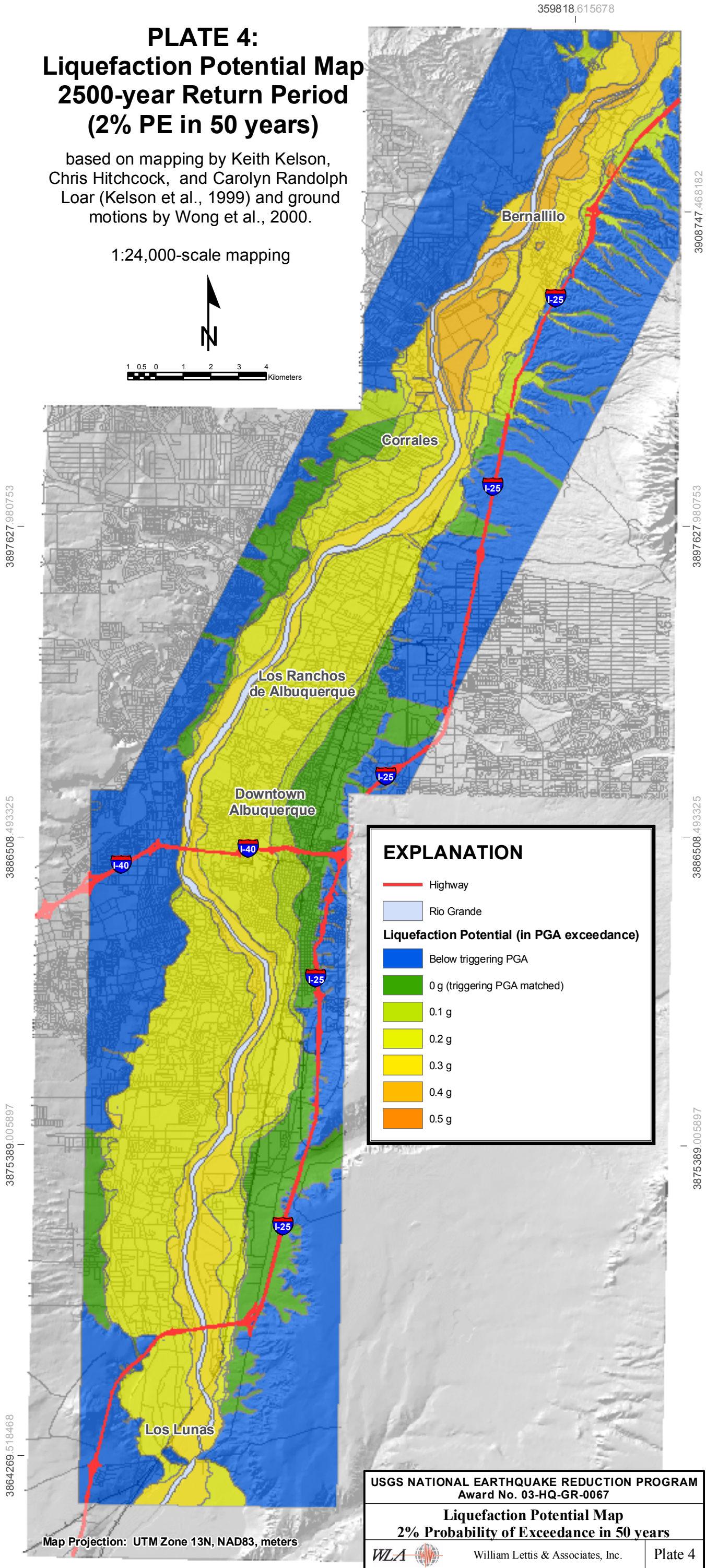
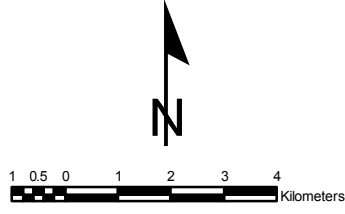
Map Projection: UTM Zone 13N, NAD83, meters

USGS NATIONAL EARTHQUAKE REDUCTION PROGRAM Award No. 03-HQ-GR-0067	
Liquefaction Potential Map Sandia-Rincon Fault Scenario (M7)	
	William Lettis & Associates, Inc.
Plate 3	

PLATE 4: Liquefaction Potential Map 2500-year Return Period (2% PE in 50 years)

based on mapping by Keith Kelson,
Chris Hitchcock, and Carolyn Randolph
Loar (Kelson et al., 1999) and ground
motions by Wong et al., 2000.

1:24,000-scale mapping



EXPLANATION

- Highway
- Rio Grande

Liquefaction Potential (in PGA exceedance)

- Below triggering PGA
- 0 g (triggering PGA matched)
- 0.1 g
- 0.2 g
- 0.3 g
- 0.4 g
- 0.5 g

Map Projection: UTM Zone 13N, NAD83, meters

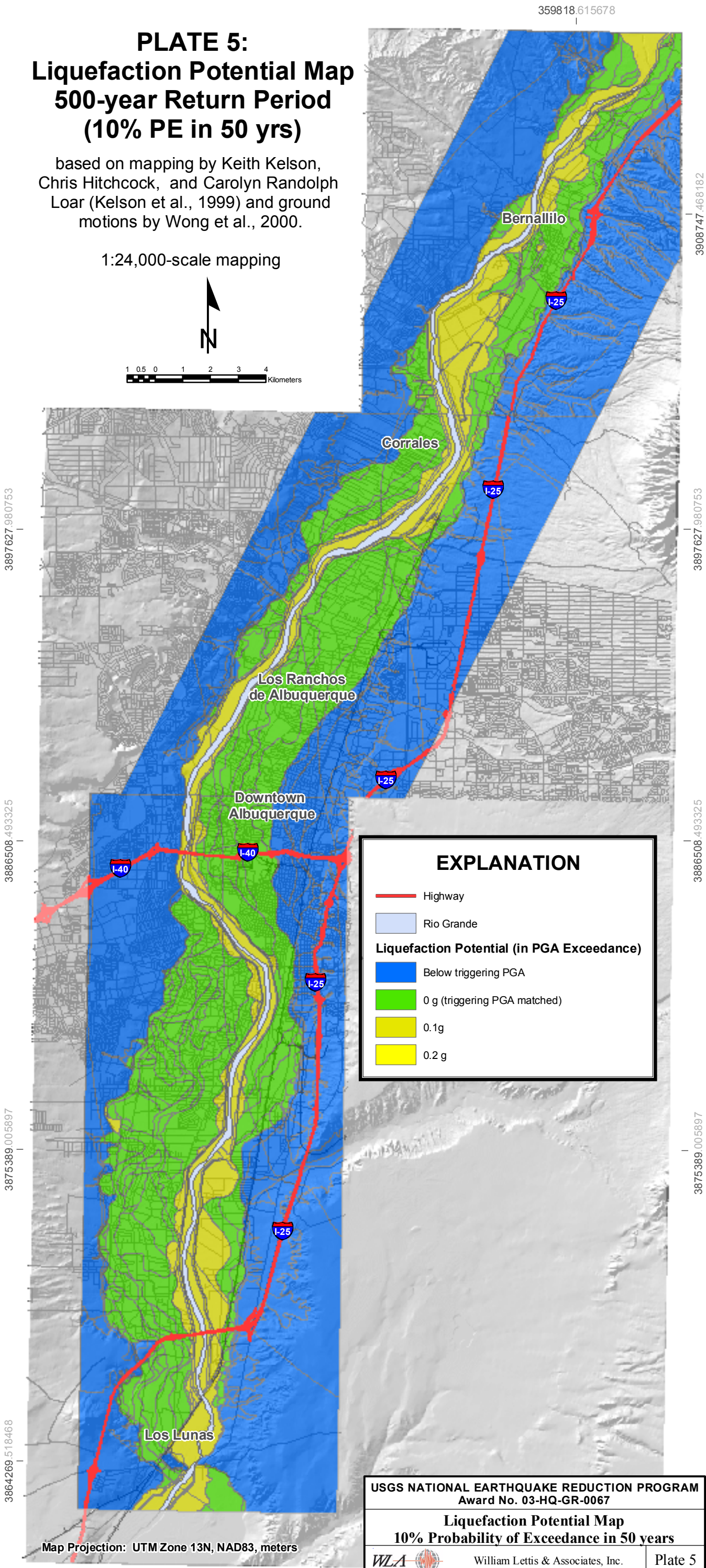
PLATE 5: Liquefaction Potential Map 500-year Return Period (10% PE in 50 yrs)

based on mapping by Keith Kelson,
Chris Hitchcock, and Carolyn Randolph
Loar (Kelson et al., 1999) and ground
motions by Wong et al., 2000.

1:24,000-scale mapping



1 0.5 0 1 2 3 4 Kilometers



EXPLANATION

- Highway
- Rio Grande
- Liquefaction Potential (in PGA Exceedance)**
- Below triggering PGA
- 0 g (triggering PGA matched)
- 0.1g
- 0.2 g

USGS NATIONAL EARTHQUAKE REDUCTION PROGRAM
Award No. 03-HQ-GR-0067

Liquefaction Potential Map
10% Probability of Exceedance in 50 years



William Lettis & Associates, Inc.

Plate 5

Map Projection: UTM Zone 13N, NAD83, meters